4 Conclusions

Thermal sprayed Al coatings showed excellent corrosion resistance in the environments investigated within the scope of the present work, even for environments exposed to H_2S with relatively high pH values. EIS and LRP were important tools in generating experimental data for the evaluation of corrosive processes. Inconsistencies were found between the values obtained from different techniques when the system was highly passive (NACE TM 0284/H_2S solution), but disappeared as the aggressiveness of the corrosive environment increased. The equivalent circuits proposed were adequate in the simulation of sprayed substrates with closed pores, as demonstrated by an excellent superimposition between experimental and theoretical plots. The presence of residual closed pores was confirmed by optical microscopy.

5 References

[1] Oden, L.L., Krug, M.P.P. & McCune, R.A. Analysis of Vapor – Aluminium – Diffused Stainless Steels. *Report of Investigations 8629*, 14p. 1989

[2] McGill, W.A. & Weinbaum, M.J. Aluminium Vapor Diffused Steels Resist Refinery Corrosion. *Material Protection and Performance*. Volume elevem, p. 28-32. 1972.

[3] Setterlund, R.B. & Prescott, G.R. Corrosion Characteristics of Iron-Aluminium and Iron-Chromium-Aluminium Alloys In High Temperature Petroleum Applications. *Official Publication National Association of Corrosion Engineers*. Vol. 17, Nº 6, p. 277-282, Houston 2 Texas 1961

[4] Weinbaum, M.J. & McGill, W.A. Alonizing to Prevent Corrosion in the HPI Sulfur Recovery Plant. *International Conference Sulphur 87*. P. 1-13, Houston-Texas 1987

[5] Joia, C., Bezerra, P., Kane, R.D., Behaviour of Thermal Spray Aluminium Coating in Wet H_2S Environments, *Corrosion – NACE 99*, paper nº 297.

[6] Thomanson, W.H. Offshore Corrosion Protection With Thermal – Sprayed Aluminum. OTC 4971, *Conoco Inc*. p.125-129, Texas May 6-9, 1985

[7] Klinge, A., Roads, K. Sprayed Zinc and Aluminium Coatings for the Protection on Structural Steel in Scandinavia. *SINTEF Report*, p. 203-213. 1976

[8] Cooper, M.T. and Thomanson, W.H. Flame Sprayed Aluminium Coatings for Corrosion Control of the Hutton Tension Leg Components. *ANTI-CORROSION*, p 4-8. July 1986

[9] ALUMINIUM – PROPERTIES AND PHYSICAL METALLURGY, *ASM*, Materials Park, Ohio, 1984

[10] Tait, W.S. An Introduction to Electrochemical Corrosion Testing for Practicing Engineers and Scientists. Chapter 04, p. 48-49, Chapter 07, p. 81-84. 1994

Corrosion protection of sintered NdFeB magnets by phosphating

A. M. Saliba-Silva[1], M. A. Baker[2], H.G. de Melo[3] & I. Costa[1]
[1] *Instituto de Pesquisas Energéticas e Nucleares, IPEN/CNEN-SP, Brasil.*
[2] *School of Mechanical and Materials Engineering, University of Surrey, Guildford.*
[3] *EPUSP - Departamento de Engenharia Química, SP, Brasil.*

Abstract

Phosphating of sintered NdFeB magnets has been studied by immersion in a solution of 0.15 M NaH_2PO_4 acidified to pH 3.7 under polarization. Cyclic polarization experiments indicated that phosphating could be assisted by polarization, with the current density decreasing as the number of polarization cycles increased. Auger electron spectroscopy (AES) and Energy Dispersive X-ray Analysis (EDX) of magnets exposed to the phosphating treatment confirmed the formation of the phosphate layer over both main phases of the specimen, namely, the magnetic (ϕ) and the Nd-rich phase. Electrochemical impedance spectroscopy (EIS) measurements performed on treated and untreated magnets immersed in synthetic saliva showed the phosphate conversion layer to improve the corrosion resistance and provided evidence of its porous nature. The phosphating procedure adopted in the present investigation is a promising surface treatment for improving the corrosion resistance of sintered NdFeB magnets.

1 Introduction

NdFeB magnets are well known for their excellent magnetic properties. They are increasingly substituting Sm-Co magnets mainly due to their lower cost and improved magnetic properties for low temperature applications. Sintered $Nd_2Fe_{14}B$ is principally used in a one particular application, the voice coil motors (VCM) of hard disk drives (HDD), which consumes about 60% of the current production [1].

Unfortunately NdFeB magnets have low corrosion resistance in various working environments [2-10], limiting their field of application [11]. To

overcome this drawback, they are usually protected by coatings. Most of the published literature concerning coatings on sintered NdFeB magnets refers to organic and metallic coatings [12-15]. Only recently, has phosphating been studied as a possible pre-treatment to increase both the corrosion resistance of the magnet [16,17] and the adherence of the coating to the substrate. Moreover, the presence of the conversion coating can improve the corrosion performance of the magnet by acting as an intermediate barrier layer in defective regions of the overlayer metallic or organic coatings.

In this study, the effect of a phosphating treatment on the corrosion resistance of a commercial sintered NdFeB magnet has been investigated using cyclic polarization and electrochemical impedance spectroscopy (EIS). The presence of phosphate on the two main phases of the magnet has also been analyzed by Auger Electron Spectroscopy and Energy Dispersive X-ray Analysis (EDX).

2 Experimental procedure

2.1 Material

A commercial sintered NdFeB magnet produced by Crucible – U.S.A., whose composition is given in table 1, was used in this investigation. The composition was determined by X-ray fluorescence analysis and atomic absorption measurments.

Table 1: Chemical composition of sintered NdFeB used in the present investigation.

Elem	Fe	Nd	B	Dy	Al	Co	Si	Cu	Nb	Na	S
Wt, %	60.6	28.3	1.0	2.1	3.7	1.3	1.4	0.2	0.2	0.4	0.2

2.2 Specimen preparation

Electrodes with an area of approximately 1.3 cm^2 were prepared by cold resin mounting. The surface treatment consisted of grinding with silicon carbide paper up to grade #1000, followed by degreasing with acetone, using an ultrasonic bath, and drying under a hot air stream.

2.3 Experimental set-up

A three electrode cell arrangement was used, with a graphite rod and a saturated calomel (SCE) as counter and reference electrode, respectively. Two types of electrochemical tests were carried out, cyclic polarization and electrochemical impedance spectroscopy (EIS). Cyclic polarization was performed using a EG&G 273A potentiostat coupled to a computer system. EIS measurements were accomplished by adding a 1255 Solartron frequency response analyser to this set-up.

2.4 Experimental procedure

To perform the cyclic polarization experiments, the sintered magnets were immersed for 30 minutes in 0.15 M NaH_2PO_4 solution acidified to pH 3.7 with H_2SO_4 and then polarized from the free corrosion potential up to 1.3 V (SCE), at which point the polarization direction was reversed.

To investigate the effect of polarization on the phosphating process, specimens were submitted to five cycles of polarization between 0.4 V and 0.6 V (SCE), immediately after immersion in the phosphating solution. This was followed by the magnet being immersed in synthetic saliva and its corrosion behavior evaluated by EIS. For comparison, EIS experiments were also performed with bare magnets in the same solution. The scanning rates used in the cyclic polarization tests were 1 mV/s, for tests carried out 30 minutes after being immersed, and 5 mV/s for experiments performed immediately after immersion.

EIS measurements were carried out in potentiostatic mode at the corrosion potential, E_{corr}. The amplitude of the perturbation signal was 10 mV, and the frequency range studied from 10^5 to 10^{-2} Hz. The solutions were all quiescent, aerated and at a temperature of (20 ± 2) ° C.

2.5 AES/EDX analysis

Chemical characterization by AES and EDX of the phosphate films formed by immersion of NdFeB magnet in 0.15 M NaH_2PO_4 solution for 24 hours was carried out using a VG Microlab mk II onto which an EDX detector had been mounted. AES/EDX point spectra were acquired using an electron beam operating at 15 keV and specimen current of 10-15 nA. The Auger spectra were acquired at a Constant Retard Ratio (CRR) of 4, step of 1 eV, for general wide scans and CRR 10, step 0.3 eV, for the phosphorous KLL region analysis.

3 Results and Discussion

Figure 1 shows a cyclic polarization curve for a NdFeB magnet after a 30 minute exposure to the phosphating solution. Low current densities, of the order of 10^{-6} $A.cm^{-2}$, were found near the corrosion potential. However, the current density increased with overpotential indicating dissolution of the magnet in the phosphating solution. Despite the response being typical of an active material, the low current densities could be indicative of a partially passive surface with active areas on it. The bottom of the small pores and the interface between the Nd rich and the ϕ phases, are the most likely active areas of the magnet.

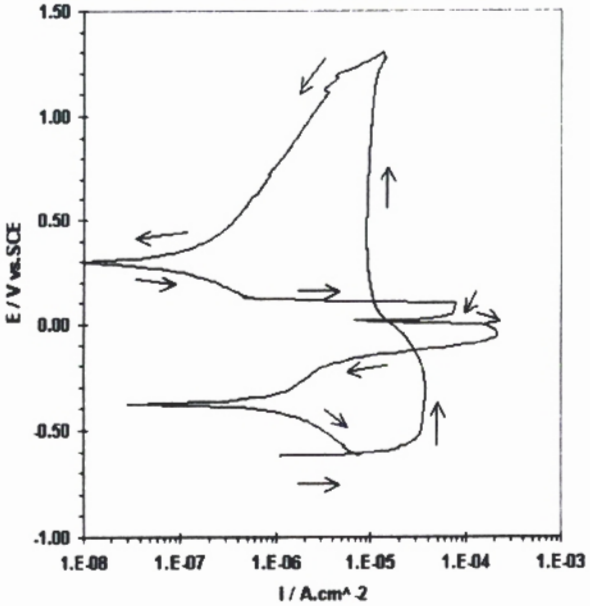

Figure 1: The cyclic polarization curve of a sintered NdFeB magnet in the phosphating solution. (Scanning rate: 1 mV/s)

A limiting current density of approximately 4 x 10^{-5} A.cm^{-2} was reached at low overpotentials (around –0.5 V), but a small reduction in current occurred at nearly –0.2 V. The reduction in the current could have been caused by precipitation of corrosion products inside the pores once its solubility limit had been exceeded, or even by the formation of a phosphating layer inside the pores. The current density stabilized at values around 10^{-5} A.cm^{-2} and it was independent of the overpotential until approximately 1.2 V, when a slight increase was observed.

A diffusion controlled process, such as diffusion through the corrosion products precipitated inside the pores, can be envisaged as responsible for this response. The polarization direction was reversed at 1.3 V, and the current measured decreased considerably during the reverse scan. During the reverse scan, the current density became negative in the potential range between 0.3 V and 0.1 V (SCE). For potentials smaller than 0.1 V (SCE) the current density became positive again and increased very rapidly, suggesting breakdown of the layer at weak areas.

Chaves and Wolynec have explained this peculiar behavior of negative current densities in cyclic polarization curves [18]. According to these authors, the passive current density does not remain constant, and the passive film, almost certainly continues to grow, rendering the film more protective. This phenomenon would produce a continuous decrease of the passive current density

during the reverse scan. At a certain potential in the reverse scan, the current density of the anodic reactions would become equal to that of the cathodic reactions, and at this point the current density would tend to zero. For lower potentials, the current density would increase again, but now with negative values, since the anodic current density would continue to decrease, while the current density of the cathodic processes would increase.

To evaluate the effect of polarization on the phosphate layer growth, a magnet immersed in the phosphating solution was subjected to five polarization cycles between 0.4 and 0.6 V. The results are presented in figure 2. For each polarization cycle, the current density decreases from the beginning to the end of the cycle. This behavior can be attributed to the formation of a more protective phosphate layer. However, as the number of cycles increased, the difference between the initial and the final current values becomes smaller, indicating that the phosphate layer tends to reach a steady state. The results suggest that polarization could assist in the phosphating treatment and reduce the time necessary to obtain a protective conversion layer on sintered NdFeB magnet.

The effect of phosphating on the morphology of the magnet surface has also been investigated. This was accomplished by applying 'nail polish' on half of the magnet surface in such a way that only the uncovered part of the surface was exposed to the phosphating solution. The magnet was then phosphated for 24 hours and after removal of the 'nail polish' using a solvent, the interface between the phosphated and untreated regions examined by Scanning Electron Microscopy (SEM). An SEM micrograph of the interfacial region (Figure 3) shows the phosphated area to exhibit a rougher morphology than the untreated surface. A rougher surface can lead to improved adhesion between the substrate and the coating. The white regions in the micrograph are the Nd rich phase, embedded in the more prevalent magnetic phase (ϕ). The sintered magnets exhibit porosity due to their manufacturing process and these pores are evident in the micrograph. Porosity and the electrical contact between phases of different electrochemical potentials are the main factors leading to the poor corrosion resistance of sintered NdFeB magnets.

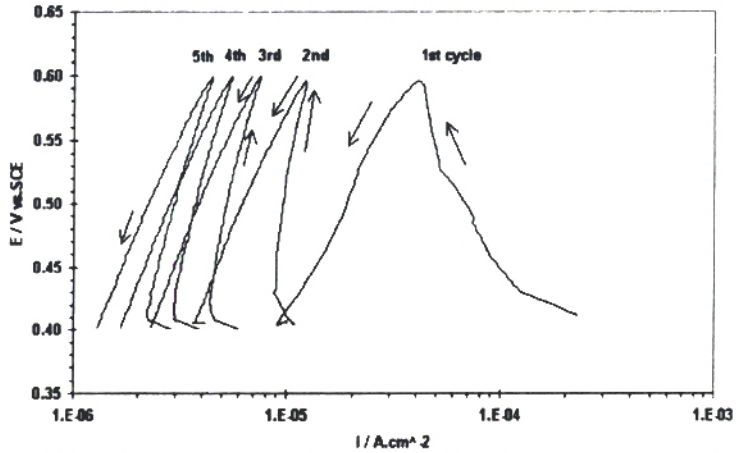

Figure 2: Cyclic polarization curves of NdFeB immediately after immersion in the phosphating solution (Scanning rate 5 mV/s).

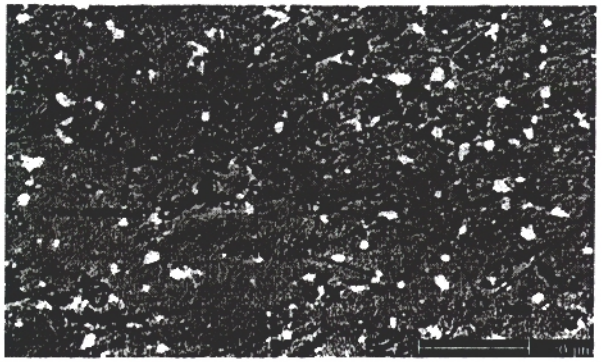

Figure 3: SEM of an NdFeB magnet showing the interface between untreated and phosphated regions.

EIS results for phosphated and untreated NdFeB magnets in synthetic saliva are presented as Nyquist diagrams in Figure 4. The improvement in the corrosion behavior of the magnets due to the presence of the conversion layer is evident from the larger Z_{RE} range obtained with phosphated electrodes.

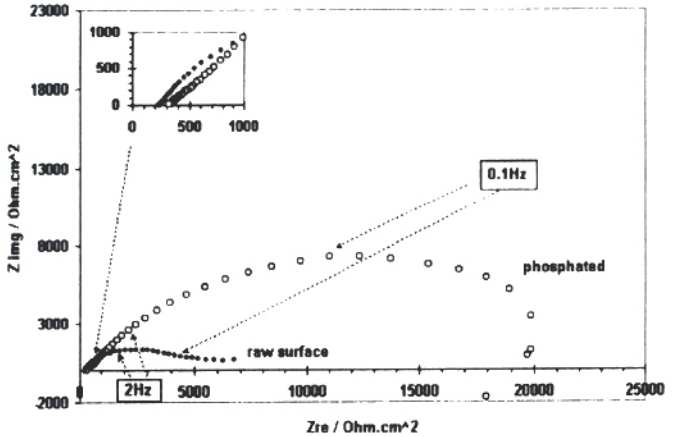

Figure 4: EIS results of phosphated and untreated Nd-Fe-B magnet in synthetic saliva.

The Nyquist plot for the untreated magnet (raw surface) consists of a depressed high frequency capacitive loop. Such a plot can be representative of complex phenomena occurring at the magnet surface as a result of the multitude of microstructural features and/or the complexity of the electrolytic solution. In the low frequency limit the imaginary part of the impedance seems to become almost constant in a certain frequency range and then to increase again in the very low frequency limit.

The plot obtained for the phosphated magnet shows a Warburg like behavior, in the high frequency region, followed by a capacitive loop. This feature is typical of a porous material with pore size distribution [19], and can be related to the porous nature of the raw sintered magnet, as already discussed.

During phosphating, the formation of the conversion layer inside the pores is not favored, giving rise to less protected regions. When the exciting a.c. signal is imposed on the electrode, it must penetrate the pore before reaching its base where the electrochemical reactions are taking place. Applying this model, the behavior of the impedance ultimately depends on the penetrability of the signal inside the pores. When the penetrability is high, the impedance behaves as a planar electrode, and the phase angle approaches –90 degrees. On the other hand, when the penetrability of the perturbing signal is smaller than the pore length, the a.c. signal detects only a part of the pore, and the phase angle tends to that found in porous electrodes, -45 degrees. Furthermore, a mixed behavior of porous and planar electrodes can also occur. This kind of behavior has been reported by Aoki *et al.* [20] for aluminum electrodes exposed in a citric acid solution. It is caused by the duplex nature of aluminum oxide, a barrier layer existing beneath a porous layer.

Concerning the behavior in the low frequency region, phosphated magnets exhibited a completely different behaviour from untreated magnets, the former

tending to inductive type behavior. With regard to the phenomena at the origin of the loops, both in the raw and phosphated magnets, interpretation is not simple due to the complex nature of the magnet surface and electrolyte, but will be addressed in forthcoming papers.

Figure 5 presents EDX spectra from the phosphated magnet taken from (a) the ϕ phase and b) the Nd rich phase. The phosphate formed after a 24 hour exposure to NaH_2PO_4 is sufficiently thick to show a strong P peak in the EDX spectra from both phases. The Auger spectra also showed the presence of strong P peaks on both phases and the Nd/Fe ratio was found to be significantly higher on the Nd rich phase compared to the ϕ phase. The P $KL_{23}L_{23}$ peak position for both phases was in the range 1848-1851 eV, consistent with the presence of phosphate [21].

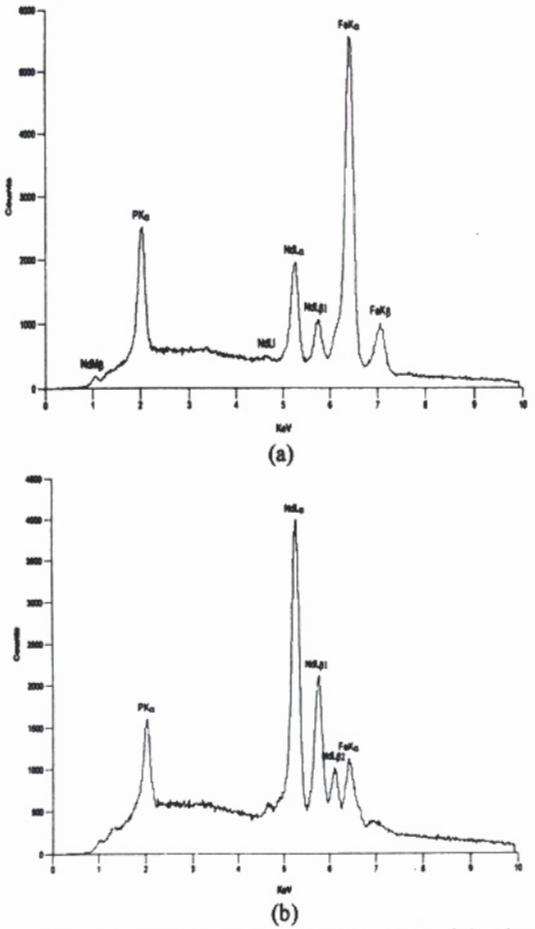

Figure 5: EDX spectra from (a) ϕ phase (b) Nd rich phase.

Conclusions

This study has shown that a phosphate treatment can be applied to sintered NdFeB magnets. Polarization can be used to reduce the time required to obtain a protective conversion layer. The improvement in the corrosion resistance of the magnets by phosphating is evident from EIS results. This data also indicates porosity in the coating, caused mainly by the porous nature of the sintered magnet surface. Auger and EDX spectra have shown the presence of the phosphate on both the Fe and Nd rich phases on the magnet surface.

References

[1] Fastenau, R.H.J. & van Loenen, E.J., Applications of rare earth permanent magnets, *J.l of Magnetism and Magnetic Materials*, **157/158** pp.1-6, 1996.

[2] Warren, G.W., Gao, Cl & Li, Q., Corrosion of NdFeB Permanent-Magnet Materials, *Journal of Applied Physics*, **70(10)**, pp.6609-6611, 1991.

[3] Hirosawa, S., Mino, S. & Tomizowa, H., Improved corrosion resistance and magnetic properties of Nd-Fe-B type sintered magnets with Mo and Co, *Journal of Applied Physics*, **(69)8**, pp. 5844-5846, 1991.

[4] Willman, C.J. & Narasimjnan, K.S.V.L., Corrosion characteristics of Re-Fe-B magnets, *Journal of Applied Physics*, **61(8)**, pp.3766-3768, 1987.

[5] Tokuhara, K. & Hirosawa, S., Corrosion resistance of Nd-Fe-B sintered magnets, *Journal of Applied Physics*, **(69)8**, pp.5521-5523, 1991.

[6] Bala, H., Pawlowska, G., Szymura, S., Sergeev, V.V. & Rabinovich, Y.M., Corrosion characteristics of Nd-Fe-B sintered magnets containing various alloying elements, *Journal of Magnetism and Magnetic Materials*, **87**, pp1255-1259, 1990.

[7] Kim, A.S., Camp, F.E. & Dulis, E.J., Effect of oxygen, carbon and nitrogen contents on the corrosion resistance of Nd-Fe-B magnets, *IEEE Transactions o n Magnetics*, **26(5)** pp.1936-1938, 1990.

[8] Tenaud, P. Lemaire, H. & Vial, F., Recent improvements in NdFeB sintered magnets, *Journal of Magnetism and Magnetic Materials*, **101**, pp.328-332, 1991.

[9] Bala, H., Pawlowska, G., Szymura, S., Sergeev, V.V. & Rabinovich, Y.M., Electrochemical corrosion characterisation of intermetallic phases occurring in Nd-Fe-B type magnets, *British Corrosion Journal*, **33(1)** pp.37-41, 1998.

[10] Dickens, Jr., E.D. & Mazany, A.M., The corrosion and oxidation of NdFeB Magnets, *Journal of Applied Physics*, **67(9)**, pp.4613-4615, 1990.

[11] Kim, A.S. & Camp, F.E., High performance NdFeB magnets, *Journal of Applied Physics*, **79(8 part 2a)**, pp.5035-5039, 1996.

[12] Cheng, C.W. & Cheng, F.T., Improvement of protective coating on NdFeB magnet by pulse neckel plating. *Journal of Applied Physics*, **83(11)**, pp.6417-6429, 1998.

[13] Qin, C.D., Li, A.S.K. & Ng, D.H.L., The protective coatings of NdFeB magnets by Al and Al(Fe), *J. of Applied Physics*, **79(8)**,pp.4854-4856, 1996.

[14] Minowa, T., Yoshikawa, M., and Honshima, M., Improvement of the corrosion resistance on Nd-Fe-B magnet with nickel plating, *IEEE Transactions on Magnetics*, **25 (5)**,pp.3776-3778, 1989.

[15] Bandeira, M.C.E., Prochnow, F. D., Costa, I., Franco, C.V. Corrosion characterization of electrodeposited organometallic films on Nd-Fe-B permanent magnets, *Key Engineering Materials*,**189-191**, pp.673-678, 2001.

[16] Costa, I., Sayeg, I.J., and Faria, R.N., The corrosion effect of RE-Iron-Boron magnets by a phosphate treatment, *IEEE Transactions on Magnetics*, **33 (5)**, pp. 3907-3909, 1997.

[17] Saliba-Silva, A.M., and Costa, I., Corrosion protection of a commercial NdFeB magnet by phosphating, *Key Engineering Materials*, **189-191**, pp. 363-368, 2001.

[18] Chaves, R., and Wolynec, S., Investigation of selective corrosion in duplex stainless steel UNS S31803 using the electrochemical potentiokinetic reactivation method – preliminary results, *Proc. of NACE-Brazil Corrosion'99*, Sao Paulo, SP, September 22nd – 24th, pp. 57-68, 1999.

[19] Song, H.-K., Jung, Y.-H., Lee, K.-H. and Dao, L.H. Electrochemical impedance spectroscopy of porous electrodes: the effect of pore size distribution, *Electrochimica Acta*, **44**, pp. 3513-3519, 1999.

[20] Aoki, I.V., Bernard, M.-C., Cordoba de Torresi, S.I., Deslouis, C., de Melo, H.G., Joiret, S., Tribollet, B. ac-Impedance and Raman spectroscopy study of the electrochemical behaviour of pure aluminium in Citric acid media, *Electrochim. Acta*, **To be published.**

[21] Franke, R., Chasse, Th., Streubel, P., Meisel, A., *Journal of Electron Spectrosc. Relat. Phenom.* **56**, 381, 1991.

Correlation between Localized Corrosion Morphology and the State of Interface of Coated TiN Thin Film

M. Ohata[1] and Yuji Kimura[2]

[1]*Graduate School, Kogakuin University, Tokyo, Japan*

[2]*Department of Environmental Chemical Engineering, Kogakuin University, Tokyo, Japan*

Abstract

Ceramic thin film was widely used due to its superior mechanical and chemical characteristics. However, defects and micro cracks were always existed from the initial stage. In corrosive environment, these defects caused the problem of localized corrosion. Moreover, the evaluations of changes of structure and the state of interface between thin film and substrate which was brought about through employing different coating methods become extremely important. Therefore, TiN thin film coating used in this study was made by two different types of coating methods, that is, plasma CVD and Dynamic Ion Mixing (DIM), which have different interfacial strength. Then, defect morphology and nm or μm orders localized corrosion generated in 3% NaCl aqueous solution was investigated by Atomic Force Microscopy (AFM). As a result, in TiN film coating made by the plasma CVD method, exfoliation of film itself was recognized from the initial stage. The crevice corrosion has been developed from this exfoliation. On the other hand, exfoliation of film itself was not confirmed in thin film coated by the DIM method. Therefore, differences in the initial state of film structure and the generated corrosion morphologies from those defects were observed. And also, improvements in corrosion and exfoliation resistances were recognized in case when superior adhesive state of interface between TiN thin film and substrate were realized.